Acid−Base Catalysis in the Mechanism of Thioredoxin Reductase from *Drosophila melanogaster*†

Hsin-Hung Huang, L. David Arscott, David P. Ballou, and Charles H. Williams, Jr.*

Department of Biological Chemistry, University of Michigan Medical School, Ann Arbor, Michigan 48109-0606

Received October 11, 2007; Revised Manuscript Received November 30, 2007

ABSTRACT: Thioredoxin reductase (TrxR) catalyzes the reduction of thioredoxin (Trx) by NADPH. Like other members of the pyridine nucleotide-disulfide oxidoreductase enzyme family, the enzyme from *Drosophila melanogaster* is a homodimer, and each catalytically active unit consists of three redox centers: FAD and an N-terminal Cys-57/Cys-62 redox-active disulfide from one monomer and a Cys-489′/Cys-490′ C-terminal redox-active disulfide from the second monomer. Because dipteran insects such as *D. melanogaster* lack glutathione reductase, thioredoxin reductase (DmTrxR) is particularly important; in addition to its normal functions, it also reduces GSSG for antioxidant protection. DmTrxR, used as a model for the enzyme from the malaria vector, *Anopheles gambiae*, has been shown to cycle in catalysis between the two-electron and four-electron reduced states, EH_2 and EH_4 [Bauer, H. et al. (2003) *J. Biol. Chem. 278*, 33020−33028]. His-464′ acts as an acid−base catalyst of the dithiol−disulfide interchange reactions required in catalysis. The H464′Q enzyme has only 2% of the wild-type activity, emphasizing the importance of this residue. The pH dependence of V_{max} for wild-type DmTrxR has pK_a values of 6.4 and 9.3 on the DmTrxR−DmTrx-2 complex, whereas H464′Q DmTrxR only has an observable pK_a at 6.4, indicating that the pK_a at pH 9.3 is contributed mainly by His-464′. The pK_a at pH 6.4 has been assigned to Cys-57 and Cys-490′; the thiolate on Cys-490′ is the nucleophile in the reduction of Trx. In contrast to wild-type DmTrxR, H464′Q DmTrxR does not stabilize a thiolate−FAD charge-transfer complex in the presence of excess NADPH. The rates of steps in both the reductive and the oxidative half-reactions are markedly diminished in H464′Q DmTrxR as compared to those of wild-type enzyme, indicating that His-464′ is involved in both half-reactions.

Thioredoxin reductase (EC 1.6.4.5) (TrxR)[1] belongs to the family of pyridine nucleotide−disulfide oxidoreductases that includes glutathione reductase (GR), lipoamide dehydrogenase, trypanothione reductase, and mercuric ion reductase (*1*, *2*). The enzyme catalyzes the reaction NADPH + H^+ + $Trx(S)_2 \leftrightarrow NADP^+ + Trx(SH)_2$ (*3*). The TrxR/Trx system has been shown to be involved in important physiological functions, such as cell growth, inflammation reactions, and apoptosis. Trx has also been shown to be an anti-apoptotic factor by binding to ASK-1 (*4*). TrxR functions as one of the major antioxidant systems in biology (*5*−*8*). Reduced thioredoxin ($Trx(SH)_2$) is able to donate reducing equivalents to both ribonucleotide reductase and methionine sulfoxide reductase to enable their catalysis (*9*, *10*). Trx is also capable of regulating the DNA binding activities of several redox-sensitive transcriptional factors, such as NF-κB, AP-1, HIF-1α, the estrogen receptor, the glucocorticoid receptor, and Ref-1 (*11*−*13*). Moreover, $Trx(SH)_2$, the product of the Trx/TrxR system, is an important antioxidant for reducing reactive oxygen species and providing reducing equivalents to thioredoxin peroxidase to reduce hydrogen peroxide (*14*).

The TrxR/Trx system has been shown to be particularly important in dipteran insects, such as *Drosophila melanogaster* and *Anopheles gambiae*, the vector of tropical malaria, because GR is absent in these organisms (*15*, *16*). Thus, to maintain a high ratio of glutathione (GSH) to glutathione disulfide (GSSG) in the cell, $Trx(SH)_2$ is necessary to reduce GSSG nonenzymatically. TrxRs from *D. melanogaster* and *A. gambiae* share 69% similarity, and the residues that contribute to the active sites of the two enzymes are virtually identical. Another indication of similarity is the fact that the substrate for the fly enzyme, DmTrx-2, is a good substrate of TrxR from *A. gambiae* and is used in the present work (*16*). As compared to DmTrx-1, DmTrx-2 is now thought to be the major form of Trx (>50 μM) in *D. melanogaster* (*17*). For these reasons, TrxR from *D. melanogaster* is an excellent model of the catalytic mechanism of the enzyme from *Diptera*.

Two forms of TrxR have been identified: low M_r TrxR with a monomer M_r of ∼35 000 and high M_r TrxR with a monomer M_r of ∼55 000 (*2*). Low M_r TrxR exists in prokaryotes, plants, and lower eukaryotes, whereas high M_r TrxR is found in higher eukaryotes. Both forms of TrxR are homodimeric flavoenzymes (*3*, *18*, *19*). The active site of low M_r TrxR contains an NADPH binding site, a FAD binding site, and one redox-active disulfide (*18*, *20*, *21*). High

† This work was supported by grants from the National Institute of General Medical Science: GM21444 (C.H.W.) and GM11106 (D.P.B.).

* Corresponding author. E-mail: chaswill@umich.edu. Tel.: (734) 647-6989. Fax: (734) 763-4581.

[1] Abbreviations: CTC, charge-transfer complex (identified as donor−acceptor); DmTrxR, thioredoxin reductase from *Drosophila melanogaster*; EH_2: two-electron reduced enzyme; EH_4: four-electron reduced enzyme; FAD, flavin adenine dinucleotide; GSH, glutathione; GSSG, glutathione disulfide; GR, glutathione reductase; PfTrxR, thioredoxin reductase from *Plasmodium falciparum*; Trx, thioredoxin; TrxR, thioredoxin reductase.

10.1021/bi702040u CCC: $40.75
Published on Web 01/23/2008

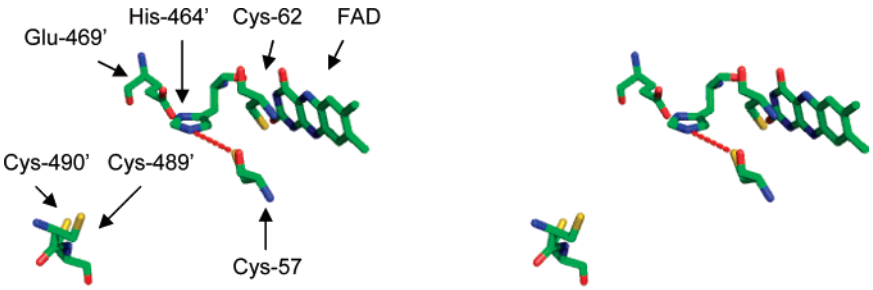

FIGURE 1: Stereoview showing the relative positions of the amino acid residues in the active site of DmTrxR. The active site contains a FAD, an N-terminal redox-active disulfide (Cys-57 and Cys-62), and a C-terminal terminal redox-active disulfide (Cys-489′ and Cys-490′). His-464′ is adjacent to the N-terminal redox-active disulfide, and the distance between NE2 of His-464′ and the sulfur atom of Cys-57 is 3.69 Å. PyMol was applied to generate the figure, and the structure used here is based on the structure of rat TrxR (pdb ID: 1H6V) (*26*).

M_r TrxR has either an additional redox-active disulfide or a selenenylsulfide formed from conserved cysteine−cysteine or cysteine−selenocysteine dyads in the neighboring subunit (*22*−*24*). It has been shown that low M_r TrxR and high M_r TrxR have different catalytic mechanisms: in low M_r TrxR, a large conformational change is required to move reducing equivalents from the apolar flavin site to the surface of the protein where Trx binds (*25*); in high M_r TrxR, this transfer is mediated by a second disulfide or selenylsulfide, and any conformational changes required are comparatively small (*22*, *26*−*28*). Comparisons to other members in the family of pyridine nucleotide−disulfide oxidoreductases reveal that the sequence of high M_r TrxR is more homologous to GR and lipoamide dehydrogenase than to low M_r TrxR (*2*, *26*). Thus, it is likely that the catalytic mechanism of high M_r TrxR is similar to that of GR and lipoamide dehydrogenase, although somewhat more complicated because of the presence of the required additional redox-active group (*22*−*24*, *27*).

The active site of TrxR from *D. melanogaster* (DmTrxR), a high M_r TrxR, contains three redox centers: FAD, an N-terminal disulfide (Cys57−Cys62) adjacent to the flavin, both from one subunit, and a second disulfide (Cys489′−Cys490′) penultimate to the C-terminal serine residue from the other subunit (*29*) as shown in Figure 1. The C-terminal polypeptide chain containing Cys-489′and Cys-490′ is flexible; it is proposed that it assumes alternate positions, first near His-464′, the acid−base catalyst, to form a mixed disulfide between Cys-57 and Cys-490′ and then at the protein surface, as shown in Figure 1, to react with Trx. A catalytic mechanism for DmTrxR has been proposed (*30*), as shown in Scheme 1. NADPH reduces FAD via hydride transfer. The resulting $FADH^-$ passes reducing equivalents to the adjacent redox-active disulfide (Cys57−Cys62), which is on the *si* side of the flavin ring, to produce a thiolate−FAD CTC involving Cys-62 (EH_2^B in Scheme 1). This nascent dithiol reduces the C-terminal cysteine pair (Cys489′−Cys490′) via a dithiol−disulfide interchange reaction. Finally, the resultant reduced C-terminal cysteine pair reduces the disulfide of the substrate, Trx. Most of these intermediate species in catalysis have identifiable spectral properties that were reported in Table 1 of McMillan et al. (*31*).

It has been shown that high M_r TrxR cycles between EH_2 and EH_4 in catalysis (*30*, *31*). As implied in Scheme 1, to initiate the interchange reaction, deprotonation of Cys-57 to form its thiolate is required for nucleophilic attack on the C-terminal disulfide, similar to what was reported for lipoamide dehydrogenase (*32*). In all members of the pyridine nucleotide−disulfide oxidoreductase family, with the exception of low M_r TrxR, a histidine residue in the active site, derived from the adjacent subunit, acts as an acid−base catalyst in the dithiol−disulfide interchange (*33*−*36*). Furthermore, in the high M_r TrxRs from humans, *D. melanogaster*, and *Plasmodium falciparum*, analogous histidine residues act as acid−base catalysts to facilitate the interchange reactions between disulfides and dithiols (*29*, *31*, *37*). On the basis of the structures of GR and the related TrxRs from rats, mice, humans, and *D. melanogaster*, it is suggested that NE2 of the imidazole ring of His-464′ is close to the interchange thiol (Cys-57) in DmTrxR (*26*, *28*, *29*, *31*, *34*−*36*, *38*). Thus, in DmTrxR, it appears that the function of His-464′ is to act as the acid−base catalyst for the dithiol−disulfide interchange reactions. In this work, the role of His-464′ was examined by measuring the pH dependence of various enzyme properties using steady-state kinetics methods, static NADPH titrations, and stopped-flow spectrophotometric methods to determine the kinetics of the reductive and oxidative half-reactions of the enzyme.

MATERIALS AND METHODS

Chemicals. NADPH, lysozyme, FAD, phenylmethylsulfonyl fluoride, leupeptin, pepstatin, tricine, boric acid, citric acid, and GSSG were purchased from Sigma-Aldrich. Nickel-nitrilotriacetic acid agarose for the purification of His-tagged proteins was from QIAGEN. Isopropyl-β-D-thiogalactopyranoside was supplied by Invitrogen. The 4−20% SDS-PAGE gels were purchased from NuSep. All other chemicals and reagents were from Fisher Scientific unless stated otherwise.

DNA Sequencing of Wild-Type DmTrxR-1 and the Histidine Mutant. The plasmids containing cDNA for wild-type DmTrxR, H464′Q DmTrxR, and DmTrx-2 were kindly provided by S. Gromer. The cDNA fragments encoding the genes of interest were inserted into the pQE-30 plasmid that allows for the expression of N-terminal His-tagged proteins. pQE-30 was obtained from QIAGEN. The sequence of each plasmid was verified by the sequencing core facility at the University of Michigan.

Preparation of Wild-Type DmTrxR-1, the Histidine Mutant, and DmTrx-2. The preparation methods were similar to those described previously (*15*, *17*). Briefly, the bacterial strain, NovaBlue from Novagene, was used for protein expression with induction by isopropyl-β-D-thiogalactopyranoside. The harvested cells were suspended in 50 mM potassium phosphate, containing 300 mM NaCl and 10 mM imidazole. In the preparation of enzymes, FAD (100 μM)

Scheme 1: Proposed Catalytic Mechanism of Wild-Type DmTrxR[a]

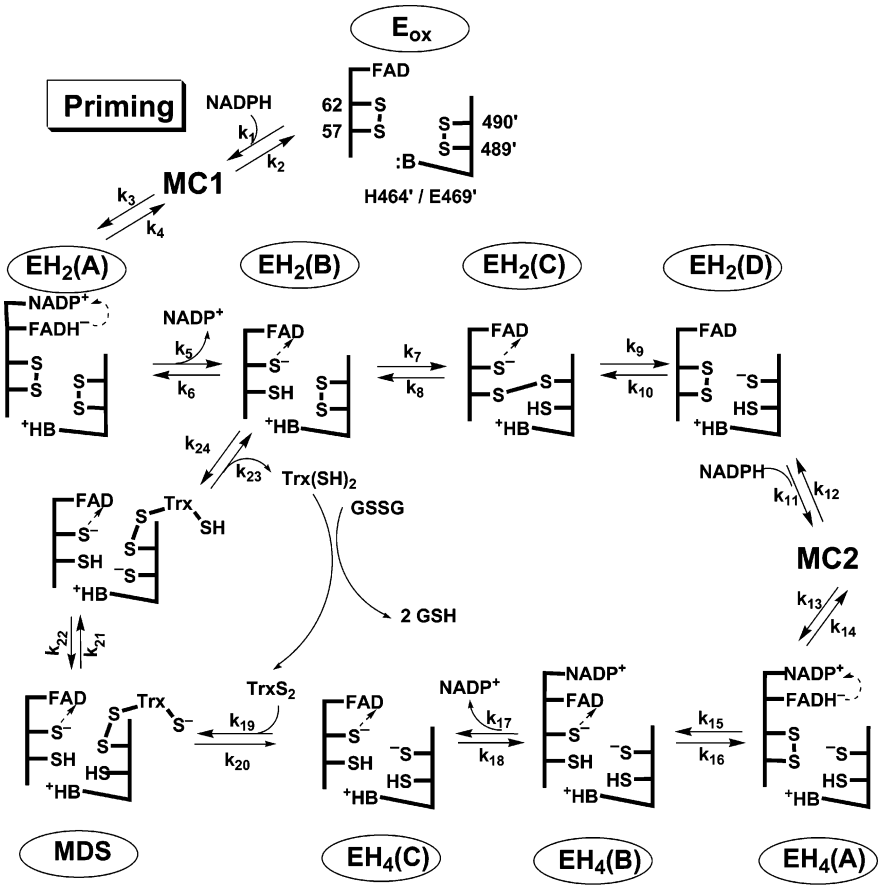

[a] Reductive half-reaction involves the steps denoted by rate constants k_1 to k_{18}, and the oxidative half-reaction involves the steps k_{19} to k_{24}. MC, Michaelis complex and MDS, mixed disulfide. Charge transfer is indicated by a dashed arrow. Residues numbered without a prime come from one monomer, and those with a prime come from the other monomer. While there is no direct evidence to show that Cys-490′ is the nucleophile that attacks the disulfide bond of DmTrx, Cys-490′ in DmTrxR occupies the same position as Sec-489′ in mammalian TrxR. Because Sec-489′ is believed to initiate nucleophilic attack on Trx, Cys-490′ in DmTrxR is thought to be the nucleophile to attack the disulfide bond of DmTrx. Data in Bauer et al. indicate that the S of Cys-490′ is attacked by Cys-57 in step k_7 and that the thiol of Cys-490′ initiates the dithiol−disulfide interchange with Trx (*30*).

was added to the lysate solution. The bacteria then were treated with lysozyme to weaken the cell walls. The protease inhibitors, phenylmethylsulfonyl fluoride, leupeptin, and pepstatin, were added to the cell lysate, which was then sonicated. The His_6-tagged proteins were applied to a nickel-nitrilotriacetic acid column and eluted by a step-gradient of imidazole. All elution buffers for the preparation of enzymes contained 100 μM FAD. The procedures for isolation of proteins were performed at 4 °C. The purity of each fraction of enzyme and of DmTrx-2 was estimated by 4−20% SDS-PAGE. The imidazole in each fraction was removed using a 10-DG desalting column from Bio-Rad to avoid the known instability of these proteins during dialysis. The concentrations of DmTrxR and of the histidine mutants, as well as of DmTrx-2, were determined spectrally using values of $\epsilon_{462nm} = 11\,900\ M^{-1}\ cm^{-1}$ for DmTrxRs and $\epsilon_{277nm} = 7320\ M^{-1}\ cm^{-1}$ for DmTrx-2 (*30*, *39*).

Determination of the Activities of DmTrxR and of the Histidine Variant. The activities of both wild-type DmTrxR and the histidine variant were measured by rates of consumption of NADPH, monitored at 340 nm in the presence of 100 μM NADPH, 50 μM DmTrx-2, and 0.3 mM GSSG in a universal buffer, pH 7.6 containing 25 mM monobasic phosphate, 25 mM borate, 25 mM tricine, and 25 mM citrate (*40*); this buffer mixture did not maintain a constant ionic strength. Results were corrected for acid-catalyzed hydrolysis of NADPH; the corrections were significant only in assays of the altered enzyme having a low activity.

Steady-State Kinetics of Wild-Type DmTrxR and the Histidine Variant over a Range of pH Values. The reaction rates of wild-type and H464′Q DmTrxR were determined at different pH values in the universal buffer by following the consumption of NADPH with various concentrations of DmTrx-2 and a fixed concentration of NADPH (100 μM) in the presence of GSSG (0.3 mM). Results were corrected for the acid-catalyzed hydrolysis of NADPH. K_m and V_{max} values were derived from a Michaelis−Menten graph of turnover numbers versus the concentration of DmTrx-2 fit to the equation for a rectangular hyperbola.

The profiles of pH were fit to eqs 1 and 2 to obtain the two pK_a value(s)

$$v = \frac{V_{max}}{\frac{10^{-pH}}{10^{-pK_{a1}}} + 1} \quad (1)$$

$$v = \frac{V_{max}}{\frac{10^{-pH}}{10^{-pK_{a1}}} + \frac{10^{-pK_{a2}}}{10^{-pH}} + 1} \quad (2)$$

Titrations of Wild-Type DmTrxR and the Histidine Variant with NADPH. The enzymes were made anaerobic in cuvettes by ~10 cycles of evacuation followed by flushing with purified argon. This procedure was performed on ice to minimize evaporation of the sample. A Hamilton titrating syringe containing an anaerobic solution of NADPH was attached to the cuvette, and small aliquots of NADPH were added during the titration. Spectra of enzymes were recorded with a Cary 3 spectrophotometer from Varian after each addition of NADPH.

Kinetics of the Reductive Half-Reactions of Wild-Type DmTrxR and the Histidine Variant Using Stopped-Flow Spectrophotometry. The reductive half-reactions of wild-type and H464′Q DmTrxR were studied by placing NADPH in anaerobic buffer in one syringe and oxidized enzyme in anaerobic buffer in the other syringe of the SF-61 DX2 stopped-flow system from Hi-Tech at 25 °C. The evolving changes in the spectra during the reaction with NADPH were observed using the photodiode array detector, and absorbance changes at single wavelengths were collected using the monochromator and a photomultiplier detector. The dead-time of the stopped-flow instrument was 1.5 ms, and the first spectrum was recorded starting 1.5 ms after the dead-time of the instrument. The apparent rate constants were derived from single-wavelength data with KinetAsyst (version 3.16) from Hi-Tech.

Kinetics of the Oxidative Half-Reactions of Wild-Type DmTrxR and the Histidine Variant Using Stopped-Flow Spectrophotometry. The oxidative half-reactions of wild-type or H464′Q enzyme were studied using the SF-61 DX 2 double-mixing stopped-flow spectrophotometer from Hi-Tech at 25 °C. Wild-type or H464′Q DmTrxR were pre-reduced with 2 equiv of NADPH anaerobically for 10 s in the first mix to produce EH_4, and the pre-reduced enzymes were mixed with various concentrations of Trx. The data were collected as described previously for the reductive half-reaction. The turbidity introduced by DmTrx-2 increased the absorbance especially between 300 and 400 nm. To correct the spectra after mixing enzymes and Trx-2, we subtracted the spectrum that was generated after mixing buffer and Trx-2 from the original spectra. The apparent rate constants of the reactions were derived from single-wavelength data with KinetAsyst (version 3.16) from Hi-Tech.

RESULTS AND DISCUSSION

Effect of pH on the Activity of Wild-Type and Variant TrxR. We investigated the pattern of macroscopic pK_a values in the H464′Q variant of DmTrxR to further understand the roles of His-464′ as an acid−base catalyst in the catalytic mechanism, in particular in the steps involving dithiol−disulfide interchange reactions (Scheme 1, steps k_7, k_9, k_{19}, and k_{23}). H464′Q DmTrxR was cloned and expressed, and its properties were compared with those of wild-type DmTrxR. The activity of H464′Q DmTrxR was only 2% that of wild-type DmTrxR under standard assay conditions ($k_{cat} = 0.33 \pm 0.02$ s^{-1} vs 15.3 ± 0.1 s^{-1}), which highlights the importance of His-464′ in catalysis. The effect of the mutation on the activity of DmTrxR is comparable to those changes observed upon analogous mutations of GR and lipoamide dehydrogenase (*41*, *42*). Because the K_m value for NADPH is less than 2 μM, its value could not be determined accurately (data not shown). Therefore, V_{max} and K_m values for the substrate, DmTrx-2, for wild-type or H464′Q DmTrxR at different pH values were determined using a fixed concentration of NADPH (100 μM). As shown in Figure 2, two apparent pK_a values are present in the pH profile of V_{max} of wild-type DmTrxR; one is at pH 6.4, and the other is at pH 9.3; however, only one pK_a value (6.4) can be discerned in the pH profile of V_{max} for H464′Q DmTrxR. The group with a pK_a of ~9.3 is missing in the complex of H464′Q DmTrxR and DmTrx-2, implying that the higher pK_a value is contributed by His-464′. This residue must be protonated to stabilize Cys-57 or Cys-490′, the likely thiolates initiating dithiol−disulfide interchange reactions (Scheme 1 and the following discussion). The high pK_a value attributed to His-464′ is reminiscent of the active site of papain; in papain, the pK_a value of His-157 is increased by the formation of an ion pair with Cys-25 (*43*, *44*).

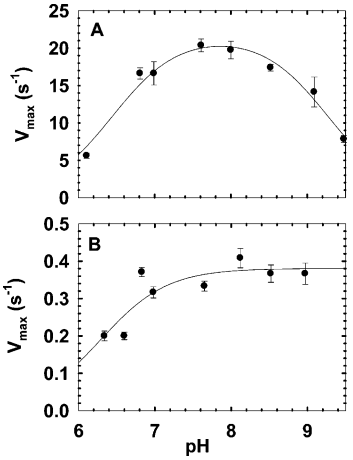

FIGURE 2: pH profiles of V_{max} for wild-type DmTrxR (A) and H464′Q DmTrxR (B). The turnover numbers were determined from the rate of NADPH consumption with various concentrations of DmTrx2 and a fixed concentration of NADPH (100 μM), in the presence of GSSG (0.3 mM) at different pH values. The K_m and V_{max} values were derived from a graph of turnover number vs concentration of DmTrx-2 fit to an equation for a rectangular hyperbola. The data were fit to eqs 1 and 2 to calculate the pK_a values.

Plots of V_{max}/K_m for wild-type DmTrxR allow for the estimation of macroscopic pK_a values of 7.0 and 8.7 on the free H464′Q DmTrxR; they are similar to those derived from plots of V_{max} versus pH. V_{max}/K_m values for H464′Q DmTrxR do not yield clear pK_a values, as shown in Figure S1 (Supporting Information). Our preliminary interpretation is that the pattern at low pH values suggests a pK_a similar to that derived for wild-type DmTrxR, but the data at high pH for the variant are ambiguous.

The most obvious assignments of the macroscopic pK_a value of 6.4 are to the two interchange thiols, Cys-57 and Cys-490′, which must be deprotonated to initiate dithiol−disulfide interchange (steps k_7, k_9 and k_{19}, k_{23}, respectively, Scheme 1). The fact that the pK_a value is observed in plots of V_{max} as well as of V_{max}/K_m reflects the complexity of the substrate, DmTrx-2, that, after binding, reacts with the enzyme to form a covalent intermediate (MDS in Scheme 1). However, it seems highly probable that Cys-57 and Cys-490′ contribute significantly to the macroscopic pK_a at pH 6.4 on the enzyme−substrate complex. There may be an analogy between the situation at this point in catalysis and

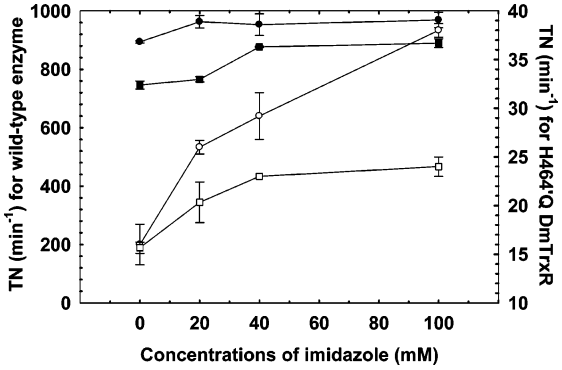

FIGURE 3: Turnover numbers of wild-type DmTrxR and H464′Q DmTrxR in the presence of imidazole-imidazolium at pH 7.5 and 8.5. (●) Wild-type enzyme, pH 7.5, left *y*-axis and (■) wild-type enzyme, pH 8.5, left *y*-axis. (○) H464′Q DmTrxR, pH 7.5, right *y*-axis and (□) H464′Q DmTrxR, pH 8.5, right *y*-axis. The concentration of imidazole, the active species, was calculated using the Henderson−Hasselbalch equation.

that existing in GR just prior to interchange with GSSG (*32*). The pK_a of the interchange thiol of GR is much higher than that of the charge-transfer thiol, and base catalysis is therefore essential to initiate interchange. The base in GR is slightly closer to the interchange thiol than to the flavin interacting thiol (*34*−*36*). His-464′ in DmTrxR would be positioned in such a way that it can interact with Cys-57 in one conformation and with Cys-490′ in a slightly different conformation (*38*). Surprisingly, this pK_a value is not changed by the mutation of His-464′, suggesting that in H464′Q DmTrxR, deprotonation of cysteine residues may be feasible at physiological pH. However, in this variant, the cysteine thiolate anions are less stable because of the loss of the stabilizing protonated His-464′. The imidazole group of His-464′ must be uncharged to assist in the formation of thiolate, and the resulting imidazolium can stabilize the thiolate by ion-pair interaction. Plots of V_{max} versus pH show that His-464′ must be protonated for maximal activity; therefore, stabilization by ion-pair formation must be more important than base catalysis.

It has been shown that imidazole will partially restore the activity in variants of thioredoxin for which the putative catalyst of thiol−disulfide interchange has been altered (*45*). Thus, it was of interest to investigate the effect of imidazole and imidazolium on the activity of the histidine variant at different pH values. The imidazole/imidazolium ratio is pH dependent; therefore, the concentration of active species, imidazole, was calculated and is indicated in Figure 3. Relatively high concentrations of imidazole partially restored the activity of H464′Q DmTrxR but had much smaller effects on wild-type enzyme. Moreover, the effect of imidazole on the activity of H464′Q DmTrxR at pH 8.5 was less than that at pH 7.5 (Figure 3). This is expected because the deprotonation of thiol groups is more favorable at higher pH values, thereby decreasing the effect of imidazole on the activity of H464′Q DmTrxR. The effects due to the addition of imidazole to the variant are consistent with the histidine residue in wild-type enzyme acting as an acid−base catalyst to facilitate the formation of a thiolate anion as well as to stabilize the thiolate by ionic interactions.

A similar example of stabilization by ionic interactions and acid−base catalysis has been studied in papain, where an ion-pair is formed between Cys-25 and His-159. Proton

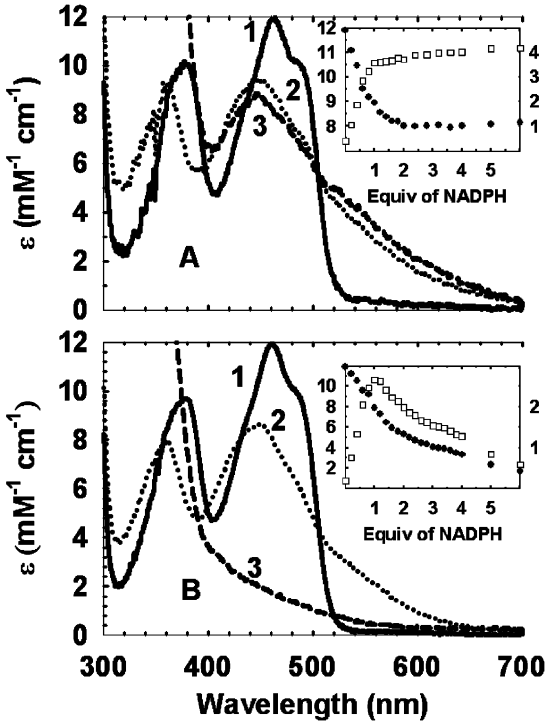

FIGURE 4: Titrations of wild-type (A) and H464′Q DmTrxR (B) with NADPH at pH 8. Spectra are as follows: 1, E_{ox}; 2, after addition of 1 equiv of NADPH; and 3, after addition of 6 equiv of NADPH. Inset: absorbance at 462 nm (●), left *y*-axis and 540 nm (□), right *y*-axis as function of equiv of NADPH added. (B) Spectra and inset as in panel A.

NMR measurements on the resting enzyme have shown that the ion-pair is favored by nearly 100% over the thiol−imidazole form (*43*, *44*). Chymotrypsin is the most commonly referred to example of an enzyme having a catalytic triad, Ser−His−Asp, and this is analogous to Cys−His−Glu in TrxR (*46*, *47*).

Titrations of Wild-Type and Variant TrxR. Static titrations of wild-type and variant TrxR with NADPH were carried out to ascertain the effects of the mutation of His-464′ on the electron distribution among the three redox centers. The titration of wild-type DmTrxR led to a blue-shift of the main flavin band (from 462 to 450 nm), and the formation of the thiolate−FAD CTC was identified by increased absorbance at 540 nm; formation of the $FADH^-$−$NADP^+$ CTC, which contributes a broad band around 670 nm, can only be observed transiently using rapid reaction techniques (*30*, *42*, *48*) (Figure 4A). After 1 equiv of NADPH was added, the wild-type enzyme was reduced to the EH_2 state (two-electron reduced enzyme), and the high absorbance at 540 nm showed that EH_2^B and EH_2^C predominated among the four EH_2 isoforms (Scheme 1). Further addition of NADPH produced EH_4^B and a small amount of EH_4^A (Scheme 1), as shown by the slight loss of flavin absorbance at 462 nm. However, in the titration of wild-type DmTrxR, the thiolate−FAD CTC observed at 540 nm reached a maximum and did not decrease, even in the presence of excess NADPH. These results are consistent with the previous findings of Bauer et al. for DmTrxR (*30*). Titrations of wild-type enzyme with NADPH at various pH values showed that the intensity and spectral characteristics of the thiolate−FAD CTC were largely unchanged between pH 7 and 9 (Figure S2 in the Supporting Information).

In stark contrast to results with wild-type DmTrxR, the spectra of reduced H464′Q DmTrxR revealed that excess NADPH fully reduced the flavin (Figure 4B cf. Figure 4A). This result indicates that the relative redox potentials of FAD, the N-terminal disulfide, and the C-terminal cysteine pair are altered in H464′Q DmTrxR from those of the wild-type enzyme. Figure 4B (inset) shows that the thiolate−FAD CTC reached a maximum and then decreased, indicating that the histidine variant was reduced beyond the EH_4 level in the presence of more than 2 equiv of NADPH, resulting in the loss of the thiolate−FAD CTC. In this family of enzymes, the redox potential of the flavin is normally lower than that of the disulfide(s); the CTC absorbance is diagnostic for the reduction of the disulfides. Even in the mammalian enzyme where the C-terminal redox-active group is a selenenylsulfide, titration with dithionite shows the uptake of three two-electron equivalents before unreacted dithionite is detected (*22*). Furthermore, the maximum amount of thiolate−FAD CTC (∼2.6 mM^{-1} cm^{-1}) observed was considerably less than that of wild-type enzyme (∼4.1 mM^{-1} cm^{-1}), again showing the importance of His-464′ for the stabilization of the thiolate−FAD CTC. This titration revealed an interesting difference between H464′Q DmTrxR and the analogous variant in the plasmodium enzyme, H509′Q PfTrxR; no thiolate−FAD CTC was observed in the latter enzyme (*31*). Overall, these results suggest that in the absence of His-464′, thiolate formation is still possible in DmTrxR but is not efficient. The effect of pH on the titration of H464′Q DmTrxR with NADPH was greater than the effect of pH on wild-type enzyme; the fraction of the thiolate−FAD CTC in H464′Q DmTrxR increased as the pH increased (Figure S3 cf. Figure S2 in the Supporting Information). This result is consistent with there being less need for stabilization of the CTC by His-464′ at high pH values.

Effect of pH on the Reductive Half-Reaction of Wild-Type and Variant DmTrxR. Because His-464′ facilitates the formation of the thiolate of Cys-57, the effects of its mutation on the reductive half-reaction should be apparent, and therefore, studies of this reaction were compared to those of wild-type DmTrxR. Figure 5A shows spectra recorded during the reductive half-reaction of wild-type DmTrxR; spectra 2−4 are of the enzyme approximately at the end of each of the three phases that were identified from the kinetic traces (Figure 5A, inset). The first phase occurred from the dead-time (1.5 ms) to ∼5 ms, the second phase was from ∼5 to ∼20 ms, and the final phase was from ∼20 to ∼300 ms. In the first phase, which was dependent on the concentration of NADPH, the absorbance at 440 nm decreased while that at 670 nm increased, showing reduction of the flavin and formation of the $FADH^-$−$NADP^+$ CTC, respectively. Thus, this step is associated with the reaction from E_{ox} to EH_2^A (Scheme 1). The mechanism proposed in Scheme 1 is based on observations made with enzyme family members lacking the C-terminal redox-active disulfide and expanded from Bauer et al. (*30*). Note that even this minimal mechanism for TrxR has at least eight reversible kinetic events associated with the reductive half-reaction (Scheme 1). The flavin was approximately 60% reduced in the first phase, but almost half of this change occurred in the dead-time of the stopped-flow instrument (∼1.5 ms). EH_2^A (Scheme 1) was the major enzyme species present at the end of this phase. In the second phase, an increased absorbance at 440 and 540 nm indicated

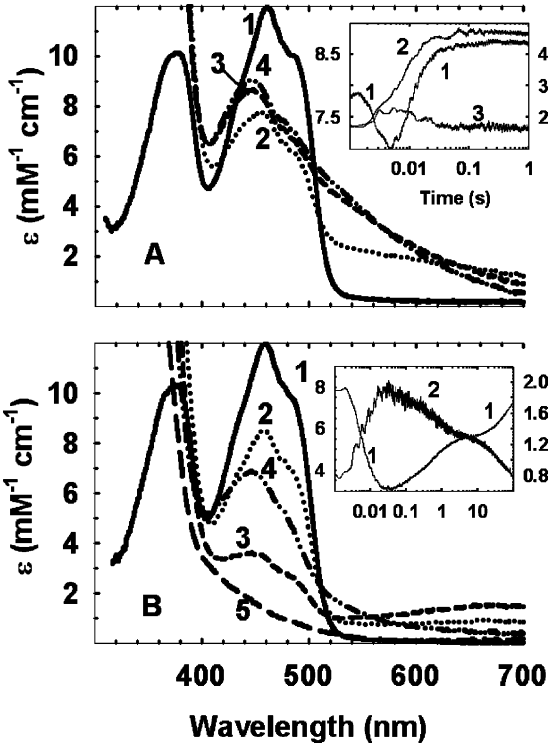

FIGURE 5: Spectra and kinetics observed in the reductive half-reactions of wild-type and H464′Q DmTrxR. All reductions were carried out at 25 °C under anaerobic conditions. (A) Reduction of wild-type DmTrxR (10 μM) with 10 equiv of NADPH at pH 8. Spectrum 1, E_{ox} and spectra 2−4, 4, 20, and 300 ms. The inset shows kinetic traces: curve 1, left *y*-axis, 440 nm; curve 2, right *y*-axis, 540 nm; and curve 3, right *y*-axis, 670 nm. (B) Reduction of H464′Q DmTrxR (10 μM) with 5 equiv of NADPH at pH 9. Spectrum 1, E_{ox} and spectra 2−5, 1 ms, 29 ms, 70 s, and 10 min. The inset shows the kinetic traces: curve 1, left *y*-axis, 450 nm and curve 2, right *y*-axis, 670 nm.

Table 1: Apparent Rate Constants Measured during Reductive Half-Reactions of Wild-Type and H464′Q DmTrxR, at Different pH Values, at 25 °C

enzymes[a]	pH	K_{dapp}-NADPH (μM)[b]	$k_{1app,max}$ (s^{-1})	k_{2app} (s^{-1})	k_{3app} [c] (s^{-1})
WT	7	13 ± 4	629 ± 56	237 ± 37	47.4 ± 9.4
WT	8	8 ± 5	562 ± 83	187 ± 12	38 ± 16
WT	9	9 ± 3	488 ± 36	107 ± 23	16.4 ± 3.5
H464′Q	7	12 ± 2	164 ± 8	0.4 ± 0.1	0.025 ± 0.015
H464′Q	8	22 ± 4	164 ± 8	1 ± 0.1	0.032 ± 0.001
H464′Q[d]	9	38 ± 6	287 ± 20	7.3 ± 0.5	1.3 ± 0.1

[a] Concentration of enzyme was 10 μM. [b] K_{dapp}-NADPH values were determined from k_{1app} and concentrations of NADPH using an equation for a rectangular hyperbola. k_{1app} reflects the reduction of the flavin. [c] k_{3app} in the reductive half-reaction of H464′Q DmTrxR at pH 7 and 8 cannot be identified in the kinetic traces. [d] Fourth phase was observed: $k_{4app} = 0.011 \pm 0.001$ s^{-1}.

that reoxidation of the flavin and formation of the thiolate−FAD CTC occurred in this phase (EH_2^A to EH_2^B in Scheme 1). The third and slowest phase may not reflect a single step; rather, it may include a dithiol−disulfide interchange (EH_2^B to EH_2^D), as well as the reaction of the enzyme with the second equivalent of NADPH (EH_2^D to EH_4^A and EH_4^B in Scheme 1). Table 1 lists the K_d values for NADPH for wild-type DmTrxR derived from the apparent first-order rate constants at each pH value, and these values are similar at pH 7−9. The rates of the second and third phases were independent of the concentration of NADPH.

The effect of pH on all the apparent rate constants is shown in Table 1. An ~2-fold decrease in the rate of the flavin reoxidation, k_{2app}, was observed with wild-type enzyme as the pH was increased and the positive charge on His-464′ decreased (Figure S1A in the Supporting Information). It is possible that this charge stabilizes the negative charge on N1 of the flavin indirectly via a solvent molecule, so that loss of the charge would promote dissociation of $NADP^+$ (EH_2^A to EH_2^B, k_5 in Scheme 1). The 3-fold decrease in the rate of the third phase as the pH was increased could have been due to a diminished need for stabilization of the charge at N1 in the reaction of the second molecule of NADPH (EH_4^A to EH_4^B, k_{15} in Scheme 1). Alternatively, in the wild-type enzyme, formation of a thiolate on either Cys-57 or Cys-62 was affected by two linked factors, pH, and the formation of an ion pair between the cysteine and the histidine residues. As the pH is increased, deprotonation of the thiol group is favored, but formation of the imidazolium group of His-464′, which is able to stabilize thiolate, is less favorable. In the reductive half-reaction of wild-type enzyme, it was observed that the second and third rate constants decreased as the pH increased. This observation suggests that for wild-type enzyme, stabilization by ion-pair formation was more significant than the increase of thiolate concentration at higher pH values, substantiating our findings in the experiment of steady-state kinetics.

The spectra recorded during the reductive half-reaction of H464′Q DmTrxR (Figure 5B) demonstrate that the reaction is very different from that of wild-type enzyme. At the end of the first phase, extending from the dead-time (1.5 ms) to ~30 ms (Figure 5B, inset, curves 1 and 2), the absorbance at 450 nm decreased (spectra 2 and 3), and absorbance appeared at 670 nm, indicating the presence of the $FADH^-$–$NADP^+$ CTC species as EH_2^A (Scheme 1). Approximately 81% of the total flavin was reduced, in contrast to wild-type DmTrxR, where only ~60% of the flavin was reduced (Figure 5A, spectrum 2 and Figure 5B, spectrum 3); reduction of the flavin beyond the EH_4 level was also observed in the static titrations (Figure 4). Because the electron transfer from reduced flavin to the N-terminal redox disulfide is decreased in the H464′Q DmTrxR variant (k_{2app}), an increased net flavin reduction would be expected in the reaction of H464′Q DmTrxR with NADPH (E_{ox} to EH_2^A in Scheme 1). From ~30 ms to ~7 s, only one significant phase was identified at pH 7 or at pH 8 (k_{2app} in Table 1), but two phases (k_{2app} and k_{3app} in Table 1) could be discerned at pH 9. In this period, the absorbance at 450 nm increased while the absorbance at 670 nm decreased, indicating reoxidation of the flavin and reduction of the adjacent disulfide without the formation of very much of the thiolate–flavin CTC. The phase seen at both pH 7 and 8 (k_{2app} in Table 1) may be associated with the steps from EH_2^A to EH_4 (Scheme 1). At pH 9, the two phases (k_{2app} and k_{3app} in Table 1) were from ~30 to ~110 ms and from ~110 ms to ~7 s. The phase characterized by k_{2app} may be associated with the transfer of electron pairs from $FADH^-$ to the N-terminal redox-active disulfide (EH_2^A to EH_2^B in Scheme 1). The phase represented by k_{3app} may not reflect a single step; it may be associated with interchange between the nascent N-terminal dithiol and the C-terminal disulfide (EH_2^B to EH_2^D in Scheme 1), as well as to the reaction of the enzyme with the second equivalent of NADPH (EH_2^D to EH_4^A and EH_4^B in Scheme 1). The phase (k_{3app} for pH 7 and 8 and k_{4app} for pH 9) from ~7 to ~60 s may not be relevant to catalysis. It is important to note that during this time period, the absorbance at 540 nm continued to slowly decrease, indicating the loss of stabilization of the thiolate–flavin CTC. After that phase, the flavin in H464′Q DmTrxR became fully bleached, as shown in Figure 5B, spectrum 5. The FAD bleached spectra can be observed in the reaction of H464′Q DmTrxR with either 5 or 10 equiv of NADPH.

The rates of all three phases decreased in the variant H464′Q DmTrxR as compared to the wild-type enzyme. As shown in Table 1, the effects on k_{2app} observed at pH 7 and 8 and on k_{2app} and k_{3app} at pH 9 were far greater than on k_{1app}. The results imply that His-464′ is important in the step in which reducing equivalents pass from the reduced flavin to the N-terminal disulfide (k_5 in Scheme 1) and the step in which reducing equivalents pass from the nascent N-terminal dithiol to the C-terminal disulfide (k_7 and k_9 in Scheme 1). The inhibitory effects due to mutation of His-464′ on these two steps were lessened at higher pH values where base catalysis is less important (Table 1). The rate of flavin reduction in H464′Q DmTrxR as compared to wild-type enzyme is affected, but to a much lesser degree, 3.8-fold at pH 7 and 1.7-fold at pH 9. Most importantly, the rates of the second and third phases increased as the pH was increased because formation of thiolate is favorable at the higher pH values. These results strongly indicate that His-464′ acts as the acid–base catalyst to facilitate thiolate formation in DmTrxR.

The K_d values for NADPH derived from the first phase are listed in Table 1; the dissociation constants of NADPH for H464′Q DmTrxR increased as the pH was raised. It has been shown that several amino acid residues are responsible for binding NADPH in rat, mouse, and human TrxR. By analogy, Arg-218 and Arg-223 in DmTrxR would form hydrogen bonds with the 2′-phosphate group of NADPH to facilitate NADPH binding to the enzyme, and Tyr-197 would be able to stack against the nicotinamide ring of NADPH, holding it in an optimal conformation to facilitate hydride ion transfer from NADPH to the flavin. It is unlikely that these amino acid residues would be affected directly by the mutation of His-464′ because the structures of rat, mouse, and human TrxRs show that they are far removed from His-464′. However, it is possible that the mutation of His-464′ does affect the positions of these amino acid residues indirectly to alter the binding of NADPH to the enzyme.

Effect of pH on the Oxidative Half-Reactions of Wild-Type and Variant TrxR. Previous studies suggested that the histidine residue analogous to His-464′ in DmTrxR is also involved in the oxidative half-reaction of PfTrxR (*31*). Therefore, the oxidative half-reactions of wild-type enzyme and H464′Q DmTrxR were studied, and the effects of pH on this half-reaction were also explored. The enzymes were prereduced to EH_4 by the addition of 2 equiv of NADPH followed by mixing with various concentrations of DmTrx-2. Figure 6A shows spectra recorded during the oxidative half-reaction of wild-type enzyme; spectrum 2 shows the prereduced enzyme (EH_4), and spectra 3 and 4 show the enzyme at the end of the two phases, identified in the kinetic traces. The reaction was finished within 10 s. Two phases were assumed in fitting the kinetic traces; the first phase from the dead-time (1.5 ms) to ~100 ms and the second

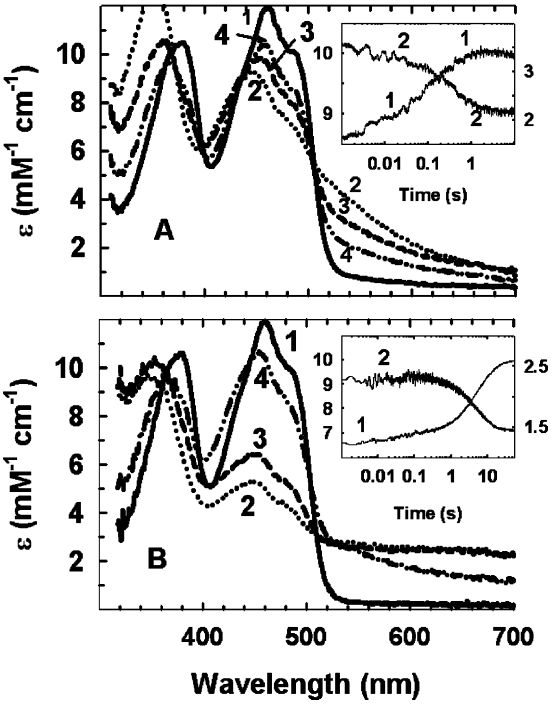

FIGURE 6: Oxidative half-reactions of wild-type and H464′Q DmTrxR at pH 7 under anaerobic conditions carried out in the double mixing stopped-flow instrument. (A) Reaction of DmTrx-2 with wild-type enzyme (10 μM) 10 s after pre-reducing with 2 equiv of NADPH in the first mix. Spectrum 1, E_{ox} as a reference and spectrum 2, pre-reduced enzyme (EH_4). Spectra were recorded at various times after mixing with 10 equiv of DmTrx-2. Spectrum 3, 116 ms and spectrum 4, 7.1 s. Kinetic traces are shown in the inset: curve 1, left *y*-axis, 450 nm and curve 2, right *y*-axis, 540 nm. (B) Reaction of DmTrx-2 with H464′Q DmTrxR (10 μM), pre-reduced with 2 equiv of NADPH. Spectrum 1, E_{ox} as a reference and spectrum 2, pre-reduced enzyme (EH_4). Spectra were recorded at various times after mixing with 10 equiv of DmTrx-2: spectrum 3, 112 ms and spectrum 4, 21 s. Kinetic traces are shown in the inset: curve 1, 450 nm, left *y*-axis and curve 2, 670 nm, right *y*-axis.

phase from ~100 ms to ~10 s are shown in Figure 6A, inset. Increases in absorbance at 450 nm and decreases in absorbance at 540 nm were observed in both phases. The first phase has only a small change in absorbance and is frequently referred to as a lag phase. This step may be attributed to the dissociation of $NADP^+$ from the enzyme. A similar first phase in the oxidative half-reaction of PfTrxR was also observed by McMillan et al. (*31*); the working temperature was 4 °C in their study of PfTrxR, whereas the temperature in this study was 25 °C. The patterns of changes in absorbance at pH 8 and 9 were similar to those at pH 7 (data not shown). As the pH was increased, the first phase decreased in rate, indicating again that the dissociation of $NADP^+$ from the enzyme may be dependent on pH. In the second phase, most of the loss of the thiolate−FAD CTC and the flavin reoxidation were observed. This phase is associated with the conversion of EH_4 to EH_2, as hypothesized for PfTrxR (*31*). Further reoxidation of the enzyme was not observed, even with 15 equiv of DmTrx-2, and this is consistent with the enzyme functioning between EH_2 and EH_4 during catalysis. The second phase showed no pH dependence (Table 2).

The spectra in Figure 6B show that the oxidative half-reaction of H464′Q DmTrxR is more complex than that of wild-type enzyme (Figure 6A); the reaction in the variant enzyme continued beyond the EH_2 stage, in contrast to wild-type enzyme, and the reaction in the variant was much slower, taking ~20 s. Three phases were distinguishable in the kinetic traces (Figure 6B, inset), unlike the two phases in wild-type enzyme: the first phase from 1.5 ms to ~0.1 s, the second phase from ~0.1 to ~1 s, and the third phase from ~1 to ~20 s. In the first and second phases, the changes in absorbance at 450 and 670 nm were small. We believe that these two phases reflect the dissociation of $NADP^+$ from the enzyme, as well as the continuous reduction of the enzyme by unreacted NADPH. The third phase, involving the largest change in absorbance at both wavelengths, shows the characteristics of enzyme reoxidation to EH_2 from EH_4, as discussed for the wild-type enzyme, but with extensive further oxidation to E_{ox} (Figure 6B). Clearly, His-464′ is involved in the oxidative half-reaction.

Table 2: Apparent Rate Constants of Oxidative Half-Reactions of Wild-Type and H464′Q DmTrxR, at Different pH Values, at 25 °C

enzymes[a]	pH	k_{1app} (s^{-1})	k_{2app} (s^{-1})	k_{3app} (s^{-1})
WT	7	28 ± 11	2.7 ± 1.4	
WT	8	18−20	2.8 ± 0.5	
WT	9	13.4 ± 4.6	2.4 ± 0.4	
H464′Q[b]	7	29.3 ± 6.2	0.5−1.5	0.17 ± 0.03
H464′Q[b]	8	24.2 ± 6.1	1.2 ± 0.4	0.17 ± 0.02
H464′Q[b]	9	ND[c]	ND[c]	0.1 ± 0.03

[a] Concentration of enzyme was 10 μM. [b] Change of absorbance in the first and second phases is small. A major absorbance change is observed in the third phase. [c] ND: not determined. The first and second phases in the oxidative half-reaction of H464′Q DmTrxR look like a lag phase; therefore, these two phases cannot be fit accurately.

On the basis of the structures of rat, mouse, and human TrxRs, the interaction between His-464′ and C-terminal redox dithiol appears to depend on the mobility of the C-terminal tail in DmTrxR that could allow the C-terminal dithiol to approach His-464′ (*26*, *28*, *29*, *38*). Thus, it is reasonable that His-464′ be involved in the oxidative half-reaction as well as the reductive half-reaction. The function of His-464′ in DmTrxR proposed by Eckenroth et al. (*29*) is based on the mechanism of GR. In the oxidative half-reaction of GR, as $_1GSSG_2$ is reduced by GR, GR-S−S-G_1 and $_2GS^-$ are produced, and His-467′ will protonate the thiolate anion, $_2GS^-$ to suppress the back reaction (*49*). Therefore, it has been proposed that like GR, the function of His-464′ in DmTrxR is to protonate the leaving group Cys-490′. Eckenroth et al. used tetrapeptides that represented the last four residues of DmTrxR to react with an enzyme in which the last four residues were removed; the leaving group of the peptides presumably will be protonated on dissociation from the enzyme. In contrast, in our enzyme system where the enzyme is in the native state, the thiol of Cys-490′ must be a thiolate to react with DmTrx-2. Therefore, we propose that the function of His-464′ in the oxidative half-reaction is to stabilize the thiolate on Cys-490′ for nucleophilic attack on the redox-active disulfide of Trx (k_{19}, Scheme 1).[2] This is consistent with our interpretation of the data in Figure S1 showing that Cys-490′ must be deprotonated and His-464′

[2] We regret that an error occurred in a previous version of Scheme 1 (*39*) reversing the proposed functions/positions of Cys-489′ and Cys-490′; data in Bauer et al. indicate that the S of Cys-490′ is attacked by Cys-57 in the step k_7 and that the thiol of Cys-490′ initiates the dithiol−disulfide interchange with Trx (*30*).

protonated for maximum activity. In addition, His-464′ may serve as the proton donor to Trx to complete the interchange. As a result, the rate of the oxidative half-reaction is less in H464′Q DmTrxR than in wild-type DmTrxR. The reasons for the small effects of pH on the reoxidation rate of H464′Q DmTrxR (k_{3app}) and wild-type enzyme (k_{2app}) are not obvious (Table 2).

CONCLUSION

Malaria is a very serious global public health problem; approximately 500 million cases of malaria are reported annually, and more than 2.5 million people, mostly children, die of this disease (*31*, *50*). The malarial protozoan parasite, *Plasmodium*, requires the mosquito vector, *A. gambiae*, for transmission of malaria to the human. Dipteran insects such as *A. gambiae* and *D. melanogaster* have an unusual need for an alternative antioxidant system because this genus lacks GR (*15*, *17*). The system consisting of Trx and TrxR has been shown to be comprised of the primary antioxidant system in *Diptera* (*15*). As mentioned in the introductory paragraphs, similarities in sequence and structure make DmTrxR a good model for the enzyme from *A. gambiae*. The long-term objective of this work was to establish differences between human TrxR, DmTrxR, and PfTrxR, victim, host−vector model, and parasite, respectively. It is hoped that these differences will be helpful to medicinal chemists in the development of inhibitors of the host−vector enzyme relative to the enzyme from the parasite.

The formation of thiolate is required for nucleophilic attack in dithiol−disulfide interchanges that are integral parts of catalysis in this family of enzymes (*1*, *45*). Although the pK_a of the thiol group of free cysteine in aqueous solution is about 8.3, considerably above physiological pH (*51*), the protein milieu can lower the pK_a value of sulfhydryl groups in the redox-active dithiol in DmTrxR. A histidine residue is conserved and has been shown to act as the acid−base catalyst in this family (*1*, *31*, *42*, *52*, *53*). Therefore, on the basis of the structures of the rat, mouse, human, and *D. melanogaster* TrxRs (*26*, *28*, *29*, *38*), His-464′, which is on the subunit adjacent to that containing the FAD and the N-terminal cysteines, is proposed to facilitate the formation of thiolate in DmTrxR. Indeed, as mentioned previously, the histidine variant, H464′Q DmTrxR, showed only 2% of the activity of wild-type enzyme, indicating that this histidine residue is crucial for the enzyme activity of DmTrxR.

How and to what extent acid−base catalysis occurs by His-464′ are questions that led to this study of the effects of pH on various enzyme properties. The effect of pH on the activity of wild-type DmTrxR defined a pK_a value of 6.4, ascribed to Cys-57 and Cys-490′, and a pK_a value of 9.3 in the DmTrxR-DmTrx-2 complex and 8.7 in free DmTrxR ascribed to His-464′. The fact that this pK_a was missing in H464′Q DmTrxR substantiates the notion that this residue is important for acid−base catalysis. The rescuing effect of imidazole on the activity of H464′Q DmTrxR corroborated the function of His-464′. In the reductive half-reaction of the enzyme, electron-pair transfers from reduced flavin to the N-terminal disulfide, and from the nascent N-terminal dithiol to the C-terminal disulfide (k_{2app} and k_{3app}), were profoundly affected in the variant, H464′Q DmTrxR. This suggested that the relative redox potentials of the three redox centers were altered by the mutation of His-464′. The rates of these two steps increased at higher pH values, as expected because base catalysis is less important at high pH values. His-464′ is also involved in the oxidative half-reaction, apparently by stabilizing the charge on Cys-490′ and by protonating Trx. Therefore, based on our evidence, it is concluded that His-464′ acts as the acid−base catalyst in both half-reactions of DmTrxR.

Glu-514′ in PfTrxR, analogous to Glu-469′ in DmTrxR (Scheme 1), has been shown to enhance the acid−base catalysis by histidine (*31*, *37*, *53*). In the study by McMillan et al., Glu-514′ was replaced by alanine, resulting in a significant decrease in active site polarity that led to enhanced thiolate−flavin charge-transfer. Future studies will investigate the effect of pH on the enhancement by Glu-469′ of acid−base catalysis by His-464′ in DmTrxR, utilizing both polar and apolar replacement residues for Glu-469′, in particular, glutamine.

ACKNOWLEDGMENT

The authors are grateful to Dr. Stephan Gromer, University of Heidelberg, and Prof. Katja Becker, University of Giesen, for supplying the vectors used in the preparation of the enzymes used in this study and in ref 39; Sailaja Pullela for her help with the preparation and characterization of the enzymes; and Dr. Raymond Trievel, University of Michigan, for critically reading the manuscript.

SUPPORTING INFORMATION AVAILABLE

pH profiles of V_{max}/K_m of wild-type and H464′Q DmTrxR (Figure S1), titration of wild-type DmTrxR with NADPH at different pH values (Figure S2), and titration of H464′Q DmTrxR with NADPH at different pH values (Figure S3). This material is available free of charge via the Internet at http://pubs.acs.org.

REFERENCES

1. Williams, C. H. (1992) *Lipoamide Dehydrogenase, Glutathione Reductase, Thioredoxin Reductase, and Mercuric Ion Reductase: A Family of Flavoenzyme Transhydrogenase*, Vol. 3, CRC Press, Inc., Boca Raton, FL.
2. Williams, C. H., Arscott, L. D., Muller, S., Lennon, B. W., Ludwig, M. L., Wang, P. F., Veine, D. M., Becker, K., and Schirmer, R. H. (2000) Thioredoxin reductase: Two modes of catalysis have evolved, *Eur. J. Biochem. 267*, 6110−6117.
3. Moore, E. C., Reichard, P., and Thelander, L. (1964) Enzymatic synthesis of deoxyribonucleotides, V. Purification and properties of thioredoxin reductase from *Escherichia coli* B, *J. Biol. Chem. 239*, 3445−3452.
4. Watson, W. H., Yang, X., Choi, Y. E., Jones, D. P., and Kehrer, J. P. (2004) Thioredoxin and its role in toxicology, *Toxicol. Sci. 78*, 3−14.
5. Mau, B. L., and Powis, G. (1992) Inhibition of cellular thioredoxin reductase by diaziquone and doxorubicin. Relationship to the inhibition of cell proliferation and decreased ribonucleotide reductase activity, *Biochem. Pharmacol. 43*, 1621−1627.
6. Bertini, R., Howard, O. M., Dong, H. F., Oppenheim, J. J., Bizzarri, C., Sergi, R., Caselli, G., Pagliei, S., Romines, B., Wilshire, J. A., Mengozzi, M., Nakamura, H., Yodoi, J., Pekkari, K., Gurunath, R., Holmgren, A., Herzenberg, L. A., and Ghezzi, P. (1999) Thioredoxin, a redox enzyme released in infection and inflammation, is a unique chemoattractant for neutrophils, monocytes, and T cells, *J. Exp. Med. 189*, 1783−1789.
7. Gromer, S., Urig, S., and Becker, K. (2004) The thioredoxin system: From science to clinic, *Med. Res. Rev. 24*, 40−89.

8. Burke-Gaffney, A., Callister, M. E., and Nakamura, H. (2005) Thioredoxin: Friend or foe in human disease? *Trends Pharmacol. Sci. 26*, 398−404.
9. Boschi-Muller, S., Olry, A., Antoine, M., and Branlant, G. (2005) The enzymology and biochemistry of methionine sulfoxide reductases, *Biochim. Biophys. Acta 1703*, 231−238.
10. Gon, S., Faulkner, M. J., and Beckwith, J. (2006) In vivo requirement for glutaredoxins and thioredoxins in the reduction of the ribonucleotide reductases of *Escherichia coli*, *Antioxid. Redox Signaling 8*, 735−742.
11. Yodoi, J., Masutani, H., and Nakamura, H. (2001) Redox regulation by the human thioredoxin system, *Biofactors 15*, 107−111.
12. Nguyen, P., Awwad, R. T., Smart, D. D., Spitz, D. R., and Gius, D. (2006) Thioredoxin reductase as a novel molecular target for cancer therapy, *Cancer Lett. 236*, 164−174.
13. Berndt, C., Lillig, C. H., and Holmgren, A. (2007) Thiol-based mechanisms of the thioredoxin and glutaredoxin systems: Implications for diseases in the cardiovascular system, *Am. J. Physiol. Heart Circ. Physiol. 292*, 1227−1236.
14. Chae, H. Z., Chung, S. J., and Rhee, S. G. (1994) Thioredoxin-dependent peroxide reductase from yeast, *J. Biol. Chem. 269*, 27670−27678.
15. Kanzok, S. M., Fechner, A., Bauer, H., Ulschmid, J. K., Muller, H. M., Botella-Munoz, J., Schneuwly, S., Schirmer, R., and Becker, K. (2001) Substitution of the thioredoxin system for glutathione reductase in *Drosophila melanogaster*, *Science (Washington, DC, U.S.) 291*, 643−646.
16. Bauer, H., Gromer, S., Urbani, A., Schnolzer, M., Schirmer, R. H., and Muller, H. M. (2003) Thioredoxin reductase from the malaria mosquito *Anopheles gambiae*, *Eur. J. Biochem. 270*, 4272−4281.
17. Bauer, H., Kanzok, S. M., and Schirmer, R. H. (2002) Thioredoxin-2 but not thioredoxin-1 is a substrate of thioredoxin peroxidase-1 from *Drosophila melanogaster*: Isolation and characterization of a second thioredoxin in *D. melanogaster* and evidence for distinct biological functions of Trx-1 and Trx-2, *J. Biol. Chem. 277*, 17457−17463.
18. Thelander, L. (1967) Thioredoxin reductase. Characterization of a homogenous preparation from *Escherichia coli* B, *J. Biol. Chem. 242*, 852−859.
19. Luthman, M., and Holmgren, A. (1982) Rat liver thioredoxin and thioredoxin reductase: Purification and characterization, *Biochemistry 21*, 6628−6633.
20. Zanetti, G., and Williams, C. H., Jr. (1967) Characterization of the active center of thioredoxin reductase, *J. Biol. Chem. 242*, 5232−5236.
21. Thelander, L. (1968) Studies on thioredoxin reductase from *Escherichia coli* B. The relation of structure and function, *Eur. J. Biochem. 4*, 407−419.
22. Arscott, L. D., Gromer, S., Schirmer, R. H., Becker, K., and Williams, C. H., Jr. (1997) The mechanism of thioredoxin reductase from human placenta is similar to the mechanisms of lipoamide dehydrogenase and glutathione reductase and is distinct from the mechanism of thioredoxin reductase from *Escherichia coli*, *Proc. Natl. Acad. Sci. U.S.A. 94*, 3621−3626.
23. Zhong, L., Arner, E. S., and Holmgren, A. (2000) Structure and mechanism of mammalian thioredoxin reductase: The active site is a redox-active selenolthiol/selenenylsulfide formed from the conserved cysteine−selenocysteine sequence, *Proc. Natl. Acad. Sci. U.S.A. 97*, 5854−5859.
24. Zhong, L., and Holmgren, A. (2000) Essential role of selenium in the catalytic activities of mammalian thioredoxin reductase revealed by characterization of recombinant enzymes with selenocysteine mutations, *J. Biol. Chem. 275*, 18121−18128.
25. Lennon, B. W., Williams, C. H., Jr., and Ludwig, M. L. (2000) Twists in catalysis: Alternating conformations of *Escherichia coli* thioredoxin reductase, *Science (Washington, DC, U.S.) 289*, 1190−1194.
26. Sandalova, T., Zhong, L., Lindqvist, Y., Holmgren, A., and Schneider, G. (2001) Three-dimensional structure of a mammalian thioredoxin reductase: Implications for mechanism and evolution of a selenocysteine-dependent enzyme, *Proc. Natl. Acad. Sci. U.S.A. 98*, 9533−9538.
27. Gromer, S., Johansson, L., Bauer, H., Arscott, L. D., Rauch, S., Ballou, D. P., Williams, C. H., Jr., Schirmer, R. H., and Arner, E. S. (2003) Active sites of thioredoxin reductases: Why selenoproteins? *Proc. Natl. Acad. Sci. U.S.A. 100*, 12618−12623.
28. Biterova, E. I., Turanov, A. A., Gladyshev, V. N., and Barycki, J. J. (2005) Crystal structures of oxidized and reduced mitochondrial thioredoxin reductase provide molecular details of the reaction mechanism, *Proc. Natl. Acad. Sci. U.S.A. 102*, 15018−15023.
29. Eckenroth, B. E., Rould, M. A., Hondal, R. J., and Everse, S. J. (2007) Structural and biochemical studies reveal differences in the catalytic mechanisms of mammalian and *Drosophila melanogaster* thioredoxin reductases, *Biochemistry 46*, 4694−4705.
30. Bauer, H., Massey, V., Arscott, L. D., Schirmer, R. H., Ballou, D. P., and Williams, C. H., Jr. (2003) The mechanism of high Mr thioredoxin reductase from *Drosophila melanogaster*, *J. Biol. Chem. 278*, 33020−33028.
31. McMillan, P. J., Arscott, L. D., Ballou, D. P., Becker, K., Williams, C. H., Jr., and Muller, S. (2006) Identification of acid−base catalytic residues of high-Mr thioredoxin reductase from *Plasmodium falciparum*, *J. Biol. Chem. 281*, 32967−32977.
32. Sahlman, L., and Williams, C. H., Jr. (1989) Titration studies on the active sites of pig heart lipoamide dehydrogenase and yeast glutathione reductase as monitored by the charge transfer absorbance, *J. Biol. Chem. 264*, 8033−8038.
33. Matthews, R. G., Ballou, D. P., Thorpe, C., and Williams, C. H., Jr. (1977) Ion pair formation in pig heart lipoamide dehydrogenase: Rationalization of pH profiles for reactivity of oxidized enzyme with dihydrolipoamide and 2-electron-reduced enzyme with lipoamide and iodoacetamide, *J. Biol. Chem. 252*, 3199−3207.
34. Pai, E. F., and Schulz, G. E. (1983) The catalytic mechanism of glutathione reductase as derived from X-ray diffraction analyses of reaction intermediates, *J. Biol. Chem. 258*, 1752−1757.
35. Karplus, P. A., and Schulz, G. E. (1987) Refined structure of glutathione reductase at 1.54 Å resolution, *J. Mol. Biol. 195*, 701−729.
36. Karplus, P. A., and Schulz, G. E. (1989) Substrate binding and catalysis by glutathione reductase as derived from refined enzyme: Substrate crystal structures at 2 Å resolution, *J. Mol. Biol. 210*, 163−180.
37. Gromer, S., Wessjohann, L. A., Eubel, J., and Brandt, W. (2006) Mutational studies confirm the catalytic triad in the human selenoenzyme thioredoxin reductase predicted by molecular modeling, *ChemBiochem 7*, 1649−1652.
38. Fritz-Wolf, K., Urig, S., and Becker, K. (2007) The structure of human thioredoxin reductase 1 provides insights into C-terminal rearrangements during catalysis, *J. Mol. Biol. 370*, 116−127.
39. Cheng, Z., Arscott, L. D., Ballou, D. P., and Williams, C. H., Jr. (2007) The relationship of the redox potentials of thioredoxin and thioredoxin reductase from *Drosophila melanogaster* to the enzymatic mechanism: Reduced thioredoxin is the reductant of glutathione in Drosophila, *Biochemistry 46*, 7875−7885.
40. Kooter, I. M., Steiner, R. A., Dijkstra, B. W., van Noort, P. I., Egmond, M. R., and Huber, M. (2002) EPR characterization of the mononuclear Cu-containing *Aspergillus japonicus* quercetin 2,3-dioxygenase reveals dramatic changes upon anaerobic binding of substrates, *Eur. J. Biochem. 269*, 2971−2979.
41. Benen, J., van Berkel, W., Dieteren, N., Arscott, D., Williams, C., Jr., Veeger, C., and de Kok, A. (1992) Lipoamide dehydrogenase from *Azotobacter vinelandii*: Site-directed mutagenesis of the His450−Glu455 diad. Kinetics of wild-type and mutated enzymes, *Eur. J. Biochem. 207*, 487−497.
42. Rietveld, P., Arscott, L. D., Berry, A., Scrutton, N. S., Deonarain, M. P., Perham, R. N., and Williams, C. H., Jr. (1994) Reductive and oxidative half-reactions of glutathione reductase from *Escherichia coli*, *Biochemistry 33*, 13888−13895.
43. Johnson, F. A., Lewis, S. D., and Shafer, J. A. (1981) Determination of a low pK for histidine-159 in the *S*-methylthio derivative of papain by proton nuclear magnetic resonance spectroscopy, *Biochemistry 20*, 44−48.
44. Lewis, S. D., Johnson, F. A., and Shafer, J. A. (1981) Effect of cysteine-25 on the ionization of histidine-159 in papain as determined by proton nuclear magnetic resonance spectroscopy. Evidence for a His-159−Cys-25 ion pair and its possible role in catalysis, *Biochemistry 20*, 48−51.
45. Chivers, P. T., and Raines, R. T. (1997) General acid/base catalysis in the active site of *Escherichia coli* thioredoxin, *Biochemistry 36*, 15810−15816.
46. Tsukada, H., and Blow, D. M. (1985) Structure of α-chymotrypsin refined at 1.68 Å resolution, *J. Mol. Biol. 184*, 703−711.

47. Craik, C. S., Roczniak, S., Largman, C., and Rutter, W. J. (1987) The catalytic role of the active site aspartic acid in serine proteases, *Science (Washington, DC, U.S.) 237*, 909−913.
48. Krauth-Siegel, R. L., Arscott, L. D., Schonleben-Janas, A., Schirmer, R. H., and Williams, C. H., Jr. (1998) Role of active site tyrosine residues in catalysis by human glutathione reductase, *Biochemistry 37*, 13968−13977.
49. Wong, K. K., Vanoni, M. A., and Blanchard, J. S. (1988) Glutathione reductase: Solvent equilibrium and kinetic isotope effects, *Biochemistry 27*, 7091−7096.
50. Linares, G. E., and Rodriguez, J. B. (2007) Current status and progresses made in malaria chemotherapy, *Curr. Med. Chem. 14*, 289−314.
51. Huber, R. E., and Criddle, R. S. (1967) Comparison of the chemical properties of selenocysteine and selenocystine with their sulfur analogues, *Arch. Biochem. Biophys. 122*, 164−173.
52. Boggaram, V., and Mannervik, B. (1978) An essential histidine residue in the catalytic mechanism of mammalian glutathione reductase, *Biochem. Biophys. Res. Commun. 83*, 558−564.
53. Brandt, W., and Wessjohann, L. A. (2005) The functional role of selenocysteine (Sec) in the catalysis mechanism of large thioredoxin reductases: Proposition of a swapping catalytic triad including a Sec-His-Glu state, *ChemBiochem 6*, 386−394.

BI702040U